Electrostatic Interactions and Conformations of Zwitterionic Pyridinium Alkanoates

Mirosław Szafran,*[,†] Zofia Dega-Szafran,[†] Andrzej Katrusiak,[†,‡] Grzegorz Buczak,[†] Tadeusz Głowiak,[§] Jerzy Sitkowski,[||] and Lech Stefaniak[||]

Faculty of Chemistry, A. Mickiewicz University, 60-780 Poznań, Poland, Instrumental Laboratory, A. Mickiewicz University, 60-780 Poznań, Poland, Faculty of Chemistry, Wrocław University, 50-383 Wrocław, Poland, and Institute of Organic Chemistry, Polish Academy of Sciences, 01224 Warsaw, Poland

Received November 11, 1997

Abstract: Conformations of flexible zwitterionic ω-pyridinium alkanoates (PBn) with *n* methylene units in the tether and their hydrates and hydrochlorides are studied in the solid state by X-ray diffraction, in aqueous solution by FT-IR and ^{1}H,^{13}C, and ^{14}N NMR spectroscopies, and in the gas phase by PM3, SAM1, and DFT calculations. PB1 and PB1·H_2O in crystals have a conformation with the $N^{+}\cdots O$ intramolecular distance of ca. 2.7 Å, while PB3·$2H_2O$ and PB10·$3H_2O$ have a *trans*-zigzag conformation and are arranged antiparallel. Structures of isolated molecules of ω-pyridinium alkanoates (PBn) and their dihydrates (PBn·$2H_2O$) and hydrochlorides (PBn·HCl) optimized using the PM3, SAM1, and DFT methods are significantly different from those observed in the crystals. In crystals, when $n \geq 2$, as a result of electrostatic interactions in the crystal lattice, the positively charged center (N^{+} atom) interacts with negative carboxyl groups, water molecules, or chloride ions of the neighboring molecules (intermolecular charge compensation), while in the gas phase only with their own (intramolecular charge compensation). In aqueous solutions, similarly as in the crystalline state, distances between the charged centers increase monotonically with increasing number of methylene units in the tether. The ^{1}H and ^{13}C NMR data suggest that polymethylene chains in PBn contain more folded (gauche) conformations than do sodium salts of carboxylic acids without a charged N^{+} atom. The SCRF calculations predict slightly longer $N^{+}\cdots C_c$ distances than those derived by Chevalier and Perchec for trimethylammonium carboxylates from ^{13}C NMR spectra. This suggests that the SCRF model underestimates contribution of the gauche conformers in aqueous solutions.

Introduction

Ammonium alkanoates (ammonioalkanocarboxylates) are zwitterions (or inner salts, or betaines), because they possess formally charged ammonium and carboxylate groups separated by one or more sp^3 carbon atoms. The chemistry of betaines has become a subject of particular interest due to their applications in biological research, especially with regard to their important role in amino acid syntheses as methyl transfer agents.[1] The crystals of many betaine complexes display interesting physical properties, exhibiting phase transitions with ferroelectric, antiferroelectric, and ferroelastic behavior.[2] Betaines containing a hydrophobic chain in the range of 8−20 carbon atoms show the unique properties characteristic for amphoteric surfactants, and their current industrial application is in toiletries and personal care products.[3]

The conformational structure of zwitterionic molecules depends on several factors. The electrostatic attraction between the two charged groups depends strongly on arm flexibility (energy differences between rotational trans and gauche isomers), bulkiness and hydration of charged groups preventing their close approach, solvent and arm electrical properties which control electrostatic attraction between the two opposite charges, and polarization of solvent around the molecule caused by the dielectric discontinuity between solvent and solute interior (image charge effect).[4−8] Electrostatic interaction is the common determinant and probably the most important element in structure−reactivity correlation in organic and biological systems. On the other hand, organic compounds are thought to be pure even though they may be a mixture of conformational isomers. This is because the isomers convert rapidly with each other at room temperature and their individual reactivities are little known.[9a] Occasionally the conformers may be stabilized in the crystallographic matrixes of polymorphic structures.[9b]

* Corresponding author. E-mail: szafran@main.amu.edu.pl.
† Faculty of Chemistry, A. Mickiewicz University.
‡ Instrumental Laboratory, A. Mickiewicz University.
§ Faculty of Chemistry, Wrocław University.
|| Institute of Organic Chemistry, Polish Academy of Sciences.

(1) Blunden, G.; Gordon, S. M. *Prog. Phycol. Res.* **1991**, *4*, 39.
(2) Schaack, G. *Ferroelectrics* **1990**, *104*, 147−158 and ref. cited therein.
(3) Domingo, X. *Amphoteric Surfactants*, Lomax, E. G., Ed., Marcel Dekker: New York, 1996; pp 75−190.
(4) Laughlin, R. G. *Langmuir* **1991**, *7*, 842−847.
(5) Chevalier, Y.; Le Perchec, P. *J. Phys. Chem.* **1990**, *94*, 1768−1774.
(6) Chevalier, Y.; Storet, Y.; Pourchet, S.; Le Perchec, P. *Langmuir* **1991**, *7*, 848−853.
(7) Weers, J. G.; Rathman, J. F.; Axe, F. U.; Crichlow, C. A.; Foland, L. D.; Scheuing, D. R.; Wiersema, R. J.; Zielske, A. G. *Langmuir* **1991**, *7*, 854−867.
(8) Kamenka, N.; Chorro, M.; Chevalier, Y.; Levy, H.; Zana, R. *Langmuir* **1995**, *11*, 4234−4240.
(9) (a) Oki, M. *Acc. Chem. Res.* **1984**, *17*, 154−159. (b) Garbauskas, M. F.; Goehner, R. P.; Davis, A. M. *Acta Crystallogr. Sect. C.* **1983**, *39*, 1684−1686.

S0022-3263(97)02069-0 CCC: $15.00
Published on Web 04/11/1998

Table 1. Experimental Conditions for the Crystal Determination and Crystallographic Data of the Investigated Compounds

	$C_5H_5N^+CH_2COO^-$	$C_5H_5N^+CH_2COO^-\cdot H_2O$	$C_5H_5N^+(CH_2)_3COO^-\cdot 2H_2O$	$C_5H_5N^+(CH_2)_{10}COO^-\cdot 3H_2O$
empirical formula	$C_7H_7NO_2$	$C_7H_9NO_3$	$C_9H_{15}NO_4$	$C_{16}H_{31}NO_5$
formula weight	137.14	155.15	201.22	317.42
temperature (K)	295(2)	293(2)	293(2)	292(2)
wavelength (Å)	0.71069	1.54178	0.71073	1.54178
crystal system	monoclinic	monoclinic	triclinic	orthorhombic
space group	$P2_1/c$	$P2_1/n$	$P\bar{1}$	$Pna2_1$
unit cell dimensions				
a (Å)	8.231(2)	7.864(2)	7.106(3)	49.104(10)
b (Å)	9.019(2)	9.915(2)	7.408(2)	7.916(2)
c (Å)	8.939(2)	9.849(2)	11.092(5)	4.6690(10)
α (deg)			88.76(3)	
β (deg)	106.21(3)	92.56(3)	80.54(4)	
γ (deg)			64.57(4)	
V (Å^3)	637.2(3)	767.2(3)	519.4(4)	1814.9(7)
Z	4	4	2	4
density (calcd) (g/cm^3)	1.429	1.343	1.287	1.162
absorption coefficient (mm^{-1})	0.106	0.897	0.101	0.695
F(000)	288	328	216	696
crystal size (mm)	0.30 × 0.30 × 0.35	0.25 × 0.25 × 0.30	0.5 × 0.3 × 0.3	0.25 × 0.10 × 0.05
θ range for data colln (deg)	2.58 to 26.99	6.34 to 72.44	1.86 to 25.06	1.80 to 69.64
index ranges	$0 \le h \le 10$, $0 \le k \le 11$, $-11 \le l \le 10$	$0 \le h \le 8$, $0 \le k \le 12$ $-12 \le l \le 12$	$-8 \le h \le 8$, $-8 \le k \le 8$, $0 \le l \le 13$	$0 \le h \le 52$, $0 \le k \le 9$, $0 \le l \le 5$
reflns collected	1039	1291	1949	1634
independent refns	1039	1291	1845 [R(int) = 0.0261]	1633
data/parameters	968/120	973/137	1843/188	1633/89
goodness-of-fit on F^2	1.076	1.065	1.071	1.157
$R1$, $wR2$ indices (all data)	0.0282, 0.0723	0.0448, 0.1168	0.0359, 0.0828	0.172, 0.267
extinction coefficient	0.71(3)	0.249(12)	0.047(7)	0
largest ΔF and hole (e Å^{-3})	0.124 and −0.129	0.198 and −0.141	0.147 and −0.118	0.525 and −0.671

Scheme 1

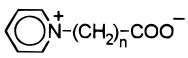

PBn; n = 1, 2, 3, 4, 5, 7, 10

In this paper the effect of the electrostatic interactions on conformations of a series of zwitterionic ω-pyridinium alkanoates, pyridine betaines, denoted as PBn (Scheme 1) of a variable-length flexible polymethylene intercharge arm (n) is examined by X-ray analyses, FT-IR and ^{1}H, ^{13}C, ^{14}N NMR spectroscopies, and semiempirical (PM3 and SAM1) and ab initio (DFT) calculations.

Experimental Section

1-(ω-Carboxyalkyl)pyridinium hydrobromides (for preparation see ref 10) were dissolved in 1:1 methanol−water mixture and treated with an ion-exchange Amberlite resin IRA-420 (OH form). The neutral eluate was evaporated to dryness under reduced pressure in a water-bath below 60 °C to afford the ω-pyridiniumalkanocarboxylates. Crude products were dried over P_2O_5 and recrystallized from acetonitrile. Yields of the HBr abstraction vary from 75 to 99%. An alternative method, described previously,[11] used propylene oxide for the preparation of carboxypyridine betaines from their hydrochlorides and gave similar results. The anhydrous PB1 was obtained by recrystallization of a sample from anhydrous methanol. All of the pyridinium betaines are hygroscopic, their melting points are: PB1, 150−151 °C, PB1.H_2O, 150−151 °C dec, PB2·H_2O 127−128 °C, [lit. 12, mp 132−134 °C], PB3·2H_2O, 103−107 °C, [lit. 13, mp 98−99 °C], PB4·2H_2O, 142−144 °C, PB5·2H_2O, 49−50 °C, PB7·2H_2O, 117−118 °C, PB10·3H_2O, 151−153 °C.

The FT-IR spectra were measured at 2 cm^{-1} resolution using a Bruker IFS 113v instrument, which was evacuated to avoid water and CO_2 absorptions. Each spectrum consists of 250 scans at 31 °C. The solution spectra (0.3 mol dm^{-3} in D_2O) were measured in a cell with CaF_2 windows, 0.025 mm thick.

The ^{1}H and ^{13}C NMR spectra were recorded on Varian Gemini 300 VT and Bruker AM 500 spectrometers, operating at 300.07 and 500.13 MHz for ^{1}H and 75.46 and 125.76 MHz for ^{13}C, respectively. The 1D, 2D, and SPT INEPT spectra were obtained with a standard Varian and Bruker softwares. The ^{1}H and ^{13}C chemical shifts were measured in D_2O relative to internal dioxane and were recalculated relative to TMS by adding 3.55 and 67.40 ppm, respectively. The concentration of the sample was 0.5 mol dm^{-3}.

The ^{14}N NMR spectra were recorded on a Bruker AM 500 spectrometer operating at 36.118 MHz frequency. The typical experimental conditions were as follows: relaxation delay 0 s, acquisition delay 0.2 s, flip angle 45°, and 2000−5000 scans. Spectra were referenced to external 0.3 M nitromethane in acetone-d_6.

X-ray diffraction analyses were carried out using a KUMA-4 diffractomer equipped with graphite monochromators. $\theta-2\theta$ scan mode was applied. All the structures were solved by direct methods[14] and refined with SHELXL-93.[15] The PB10·3H_2O structure was refined to relatively low convergence due to the low quality of the twinned sample crystals. Low precision of diffraction data is often characteristic for the molecular crystals built of long molecular chains.[16,17] However, the molecular aggregation pattern of the molecules arranged in the crystal lattice and the molecular conformation are clearly revealed by these results. In this analysis the C, N, and O atoms were refined with isotropic temperature factors,

(10) Dega-Szafran, Z.; Szafran, M. *Bull. Pol. Acad. Sci. Chem.* **1995**, *43*, 295−302.
(11) Dega-Szafran, Z.; Kowalczyk, I.; Szafran, M. *Bull. Pol. Acad. Sci. Chem.* **1995**, *43*, 303−312.
(12) Gresham, T. L.; Jansen, J. E.; Shaver, F. W.; Bankert, R. A.; Fiedorek, F. T. *J. Am. Chem. Soc.* **1951**, *73*, 3168−3171.
(13) Lukeš, R.; Pliml, J. *Collect. Czech. Chem. Commun.* **1956**, *21*, 1602−1606.
(14) Sheldrick, G. *SHELXS-86. A Program for Crystal Structure Determination.* University of Göttingen, 1986.
(15) Sheldrick. G. *SHELXL-93. Program for Refinement of Crystal Structures.* University of Göttingen, 1983.
(16) Nyburg, S. C.; Gerson, A. R. *Acta Crystallogr. Sect. B* **1992**, *B48*, 103−106.
(17) Ratajczak-Sitarz, M.; Katrusiak A.; Gdaniec, M. *Pol. J. Chem.* **1992**, *66*, 1169−1174.

and the hydrogen atom positions were calculated from the zwitterion geometry; the hydrogen atoms of three water molecules were not included in the final model. For the other structures all C, N, and O atoms were refined with anisotropic temperature factors, and all the H atoms were located from difference Fourier maps and refined with isotropic temperature factors. The crystal data and details concerning data collection and structure refinement are given in Table 1.

Structures and energies were calculated by means of the PM3[18] and SAM1[19] semiempirical methods, as implemented in the AMPAC 5.0 and MOPAC V5.0 program packages.[20,21] Planarity of the pyridine ring was assumed, while the other geometrical parameters were optimized (with keyword PRECISE). To avoid false minima, several input starting geometries were used corresponding to different conformations about the methylene groups between the charged centers. In some folded structures one of the α-C−H bond of pyridine was elongated up to 1.28 and 1.4 Å in PM3 and SAM1 calculations, respectively, or even abstracted. This is clearly an artifact of these methods which overestimates attractive interaction between the atoms H_α and O−C. Thus both PM3 and SAM1 calculations were run twice: (1) with all the C−H bonds optimized, and (2) with two α-C−H bond lengths fixed, where $C_{2'}-H = C_{6'}-H + (C_{3'}-H - C_{5'}-H)$; where the difference $C_{3'}-H - C_{5'}-H$ varies from 0.001 to 0.002 Å. The ab initio calculations were performed with the GAUSSIAN 94 program package.[22] The molecular parameters were optimized in the ab initio calculations at DFT[23] level using the split-valence polarized 6-31G(d,p) basis set[24] and the exchange functional proposed by Becke[25] and the correlation functional proposed by Lee et al.[26] (BLYP) were used, and all the electrons were correlated.

The solvent effect was taken into account by using the self-consistent reaction field (SCRF) method.[27] The SCRF method was implemented in the MOPAC program. The cavity radius a_o was estimated from the geometries of all trans and all gauche conformers.

Results and Discussion

Nomenclature of betaines is based on the selection of a parent ion molecule that includes one of the charged groups. The IUPAC system allows either ions to serve as a parent ion molecule. In this paper the COO^- ion was selected, but methylene groups are numbered from nitrogen atom toward the carboxylate group (Figure 1). The letter *n* denotes the number of methylene tether groups in betaines and their hydrohalides.

X-ray Diffraction. Figure 1 shows the betaines and the closest water molecules, as well as the numbering of the atoms. Bond distances, bond angles, and selected torsional angles are deposited and may be obtained on request. The geometry of the pyridine rings is in a good agreement with that reported for other betaines in the literature.[28] The geometry of the carboxylate group varies on hydratation and with the number of methylene groups between the charged fragments. This is attributed to the hydrogen bond effect. The dihedral angles indicate that the tether group assumes roughly a trans-zigzag conformation.

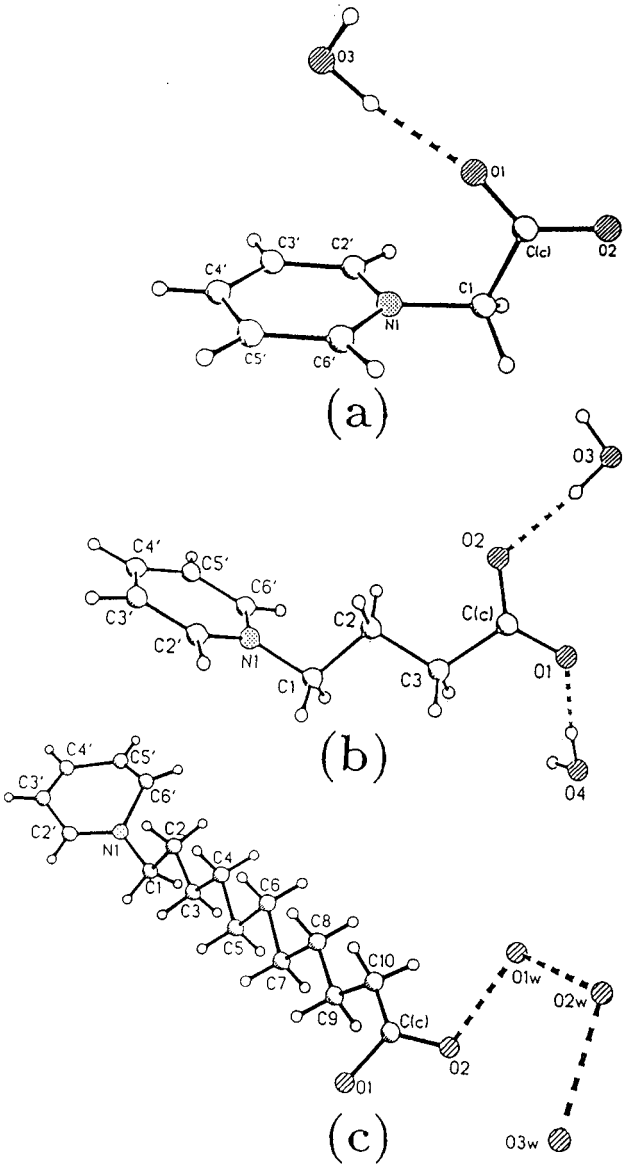

Figure 1. Perspective views showing formula units in the hydrated crystals of (a) PB1·H_2O, (b) PB3·$2H_2O$, and (c) PB10·$3H_2O$.

Figure 2 shows the molecular arrangements in the crystal lattices. In hydrates the water molecules form hydrogen bonds with carboxylate groups. The intramolecular and interatomic distances listed in Table 2 show that the former increases with *n*, while the latest are almost independent of *n*. The torsion angles and interatomic distances in crystals of PB3·$2H_2O$ are similar to those of carnitine hydrochloride[29a,b] and 2-carboxy-*N*,*N*,*N*-trimethylethanamminium bromide monohydrate[29c] because of similar *trans*-zigzag main chain conformation.

(18) Stewart, J. J. P. *J. Comput. Chem.* **1989**, *10*, 221−264.
(19) Dewar, M. J. S.; Jie, C.; Yu, J. *Tetrahedron* **1993**, *49*, 5003−5038.
(20) *AMPAC 5.0*, Semichem, Shawnee, KS 66216, 1994.
(21) *MOPAC V5.0*. Stewart, J. J. P. *QCPE Bull.* **1989**, *9*, 10; QCPE program no 455.
(22) Frisch, M. J.; Trucks, G. W.; Head-Gordon, M.; Gill, P. M. W.; Wong, M. W.; Foresman, J. B.; Johnson, B. G.; Schlegel, H. B.; Robb, M. A.; Replogle, E. S.; Gomperts, R.; Andres, J. L.; Raghavachari, K.; Binkley, J. S.; Gonzalez, C.; Martin, R. L.; Fox, D. J.; Defrees, D. J.; Baker, J.; Stewart, J. J. P.; Pople, J. A. *Gaussian 94*, Revision B, Gaussian, Inc., Pittsburgh, PA, 1994.
(23) Kohn, W.; Sham, L. J. *Phys. Rev.* **1965**, *A140*, 1133−1138.
(24) Hariharan, P. C.; Pople, J. A. *Theor. Chim. Acta*, **1973**, *28*, 213−222.
(25) Becke, A. D. *Phys. Rev.* **1988**, *A38*, 3098−3100.
(26) Lee, C.; Yang, W.; Parr, R. G. *Phys. Rev.* **1988**, *B37*, 785−789.
(27) (a) Tapia, O.; Goscinski, O. *Mol. Phys.* **1975**, *29*, 1653−1661. (b) Tapia, O.; Silvi, B. *J. Phys. Chem.* **1980**, *84*, 2646−2658. (c) Tapia O. In *Molecular Interactions*; Ratajczak, H., Orville-Thomas, W. J., Eds.; Vol. 3, J. Wiley: Chichester, 1982; pp 47−117.
(28) (a) Chen, X.-M.; Mak, T. C. W. *J. Mol. Struct.* **1990**, *221*, 265−269. (b) Chen, X.-M.; Mak, T. C. W. *Acta Crystallogr. Sect. C* **1994**, *C50*, 1807−1809. (c) Wu, D.-D.; Mak, T. C. W. *J. Mol. Struct.* **1995**, *372*, 187−193.

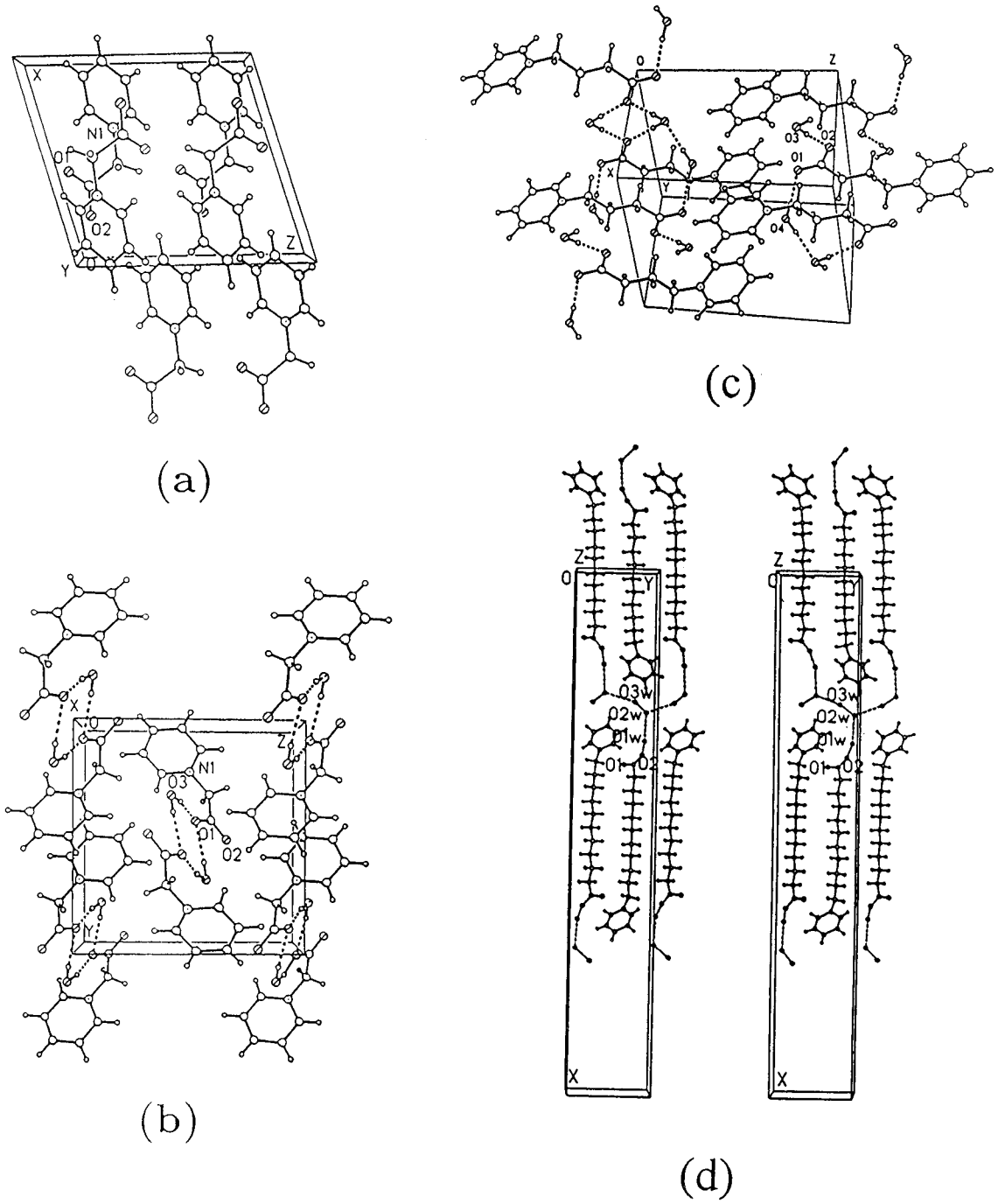

Figure 2. Stereoview of the crystal structures of (a) PB1, (b) PB1·H_2O, (c) PB3·$2H_2O$, and (d) PB10·$3H_2O$ as determined from the X-ray diffraction analyses.

Conformation of pyridine betaine and its hydrate can be described with reference to two planes: A of atoms N, C(2′), C(6′), and B of atoms O(1), C(c), O(2), and C(1). The dihedral angles between planes A and B are 80.1(1)° and 84.5(1)° for PB1 and PB1·H_2O, respectively.

There are no unusual short contacts in the investigated crystals. In the crystalline state the zwitterionic molecules are arranged in the manner minimizing the electrostatic interactions between the charged centers. Both PB1 and PB1·H_2O molecules assume a conformation (Figures 2a and 2b), with one of the oxygen atoms located closer, at about 2.7 Å, to the nitrogen atom, while the distance from the nitrogen to the second oxygen atom exceeds 3.6 Å in both cases. The nonsolvated molecules are stacked head-to-tail, so that the N^+ atom has two COO^- groups of the neighboring molecules on both sides at about 3.75 Å; these columns are arranged along [*y*], as shown in Figure 2a. There are fewer intermolecular short contacts between the N^+ and COO^- groups in PB3·$2H_2O$. Only the O(2) atom, which is not involved in the hydrogen bonds with water molecules, has short contacts of 3.75 Å with the N^+ atom, while the lone-electron pairs of the water molecules are directed toward the N^+ atoms, as can be seen in Figure 2b. Even fewer intermolecular

(29) (a) Tomita, K.-I.; Urabe, K.; Kim, Y. B.; Fujiwara, T. *Bull. Chem. Soc. Jpn.* **1974**, *47*, 1988−1993. (b) Destro, R.; Heyda, A. *Acta Crystallogr. Sect. B* **1977**, *B33*, 504−509. (c) Chen, X.-M.; Mak, T. C. W. *J. Mol. Struct.* **1991**, *245*, 301−306.

Table 2. Selected Intramolecular and the Shortest Intermolecular Nonbonding Distances (Å) Involving Atoms C(c), N^+, O(1), O(2), and Water Oxygen Atoms in the Crystals of Zwitterions (see Figure 1)

distance	$C_5H_5N^+CH_2COO^-$	$C_5H_5N^+CH_2COO^-\cdot H_2O$	$C_5H_5N^+(CH_2)_3COO^-\cdot 2H_2O$	$C_5H_5N^+(CH_2)_{10}COO^-\cdot 3H_2O$
		Intramolecular		
$N^+\cdots C(c)$	2.518(2)	2.508(4)	5.030(4)	13.86(2)
$N^+\cdots O(1)$	2.720(2)	2.704(3)	6.120(4)	14.01(2)
$N^+\cdots O(2)$	3.620(2)	3.600(3)	5.131(4)	14.91(2)
		Intermolecular[a]		
$N^+\cdots C(c)$	4.209(2) (1-x; 0.5+y; 1-z)	4.417(4)(-x; 1-y; 1-z)	4.526(4) (1-x; 1-y; 2-z)	3.82(2) (1-x; 1-y; −0.5+z)
$N^+\cdots O(1)$	3.787(2) (1-x; 0.5+y; 0.5-z)	4.833(3) (-x; 1-y; 1-z)	3.983(3) (-x; 1-y; 2-z)	2.73(2) (1-x; 1-y; −0.5+z)
$N^+\cdots O(2)$	4.442(2) (1-x; 1-y; -z)	3.753(3) (-x; 1-y; 1-z)	4.761(4) (1-x; 1-y; 2-z)	3.98(2) (1-x; 2-y; −0.5+z)
$N^+\cdots O(3)$		4.001(3) (x; y; z)	4.166(3) (1-x; 1-y; 2-z)	
$N^+\cdots O(4)$			4.312(4) (1-x; 1-y; 2-z)	
$N^+\cdots N^+$	4.946(2) (1-x; 1-y; 1-z)	4.114(3) (-x; -y; 1-z)	5.187(5) (-x; 2-y; 3-z)	4.67(1) (x; y; z+1)
C(c)···C(c)	4.218(3) (1-x; 1-y; -z)	3.430(4) (-x; 1-y; 1-z)	4.289(4) (1-x; 1-y; 2-z)	4.67(1) (x; y; z+1)
O(1)···O(1)	3.936(2) (1-x; 1-y; -z)	3.873(3) (1-x; 1-y; 1-z)	5.800(4) (1-x; 1-y; 2-z)	4.67(1) (x; y; z+1)
O(2)···O(2)	3.974(2) (-x; 1-y; -z)	3.812(3) (-x; 1-y; 1-z)	4.982(4) (1-x; 1-y; 2-z)	4.67(1) (x; y; z+1)
O(1)···O(2)	4.288(2) (1-x; 1-y; -z)	3.615(3) (-x; 1-y; 1-z)	4.940(3) (1-x; 1-y; 2-z)	4.24(2) (x; y; z-1)
$N^+\cdots O(1W)$		4.001(3) (x; y; z)	7.658(5) (x; y; z)	3.71(2) (1-x; 2-y; z-0.5)
$N^+\cdots O(2W)$			6.942(4) (x; y; z)	5.03(2) (1-x; 2-y; z-0.5)
$N^+\cdots O(3W)$				4.81(2) (x-0.5; 1.5-y; z)

[a] symmetry code of the second atom in parantheses.

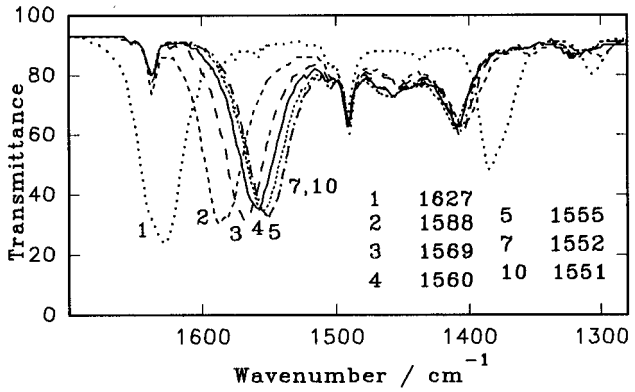

Figure 3. FT-IR spectra of pyridine betaines with various polymethylene bridges in D_2O.

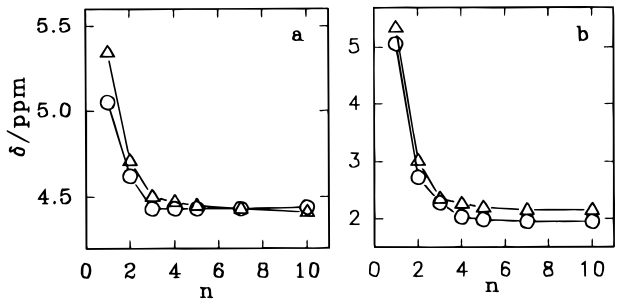

Figure 4. Effect of the polymethylene bridges length on the proton chemical shift of pyridine betaines (○) and their hydrobromides (Δ) in D_2O: (a) $N^+C\mathbf{H}_2$ and (b) $C\mathbf{H}_2COO^-$. Data for hydrobromides are taken from ref 21

contacts are observed in PB3·$2H_2O$, where both oxygen atoms of the COO^- group are hydrogen-bonded to water molecules (Figure 2c). Both PB3·$2H_2O$ and PB10·$3H_2O$ have extended conformations which prevent short intramolecular contacts between the charged groups. In PB10·$3H_2O$ the molecules are arranged antiparallel; only one carboxylate oxygen O(2) is hydrogen-bonded to a water molecule, O(1W), as shown in Figure 2d, and similarly as in PB1·H_2O only the carboxylate oxygen atom not involved in hydrogen bonds, the O(1) atom, has short intermolecular contacts of 2.73(2) Å to the N^+ atom of the neighboring molecule (Table 2). The crystal packing of the zwitterions in the investigated structures can be characterized as governed by electrostatic interactions between the charged groups. In PB1 both intra- and intermolecular electrostatic interactions can be identified from short nonbonding contacts (Table 2). When longer $(CH_2)_n$ chains separate the charged groups, the molecules assume extended conformations, and their polar groups are compensated by the close vicinity of the opposite polar groups of neighboring molecules, or by the appropriately oriented water-molecule dipoles.

FT-IR Studies. Figure 3 shows the spectra in the 1700−1250 cm^{-1} region. The major bands of interest are the antisymmetric and symmetric stretching bands of the carboxylate groups. The frequency of the $\nu_{as}COO$ band clearly depends on the length of the tether group and varies from 1627 to 1551 cm^{-1} in D_2O (Figure 3) and from 1636 to 1564 cm^{-1} in the solid state. Similar behavior of carboxylate groups has been observed in (*N*-dodecyl-*N*,*N*-dimethylammonio)alkanoates.[7] The frequency lowering of the $\nu_{as}COO$ band reflects the symmetry increase of the group and can be explained by the chemical effect of the larger charge separation proportional to *n*. The $\nu_s COO$ frequency is less affected by the length of the tether group, except when $n = 1$.

^{1}H NMR Studies. Deposited proton chemical shift assignments were based on 2D COSY[30] experiments in which the proton−proton connectivities are observed through the off-diagonal peaks in the counter plot. Figure 4 shows a variation of the selected proton chemical shifts with the increasing number of methylene groups. In 1-alkylpyridinium salts, protons of the $N^+C\mathbf{H}_2$ group are slightly deshielded on elongation of the carbon chain,[31] while in the investigated betaines and their hydrobromides, these protons are shielded with the increasing number of methylene groups. Also the protons of the CH_2COO group are shielded with the increasing number of methylene groups. This suggests that the polymethylene chain is not significantly folded in D_2O solution.

In all investigated pyridine betaines, protons of the $N^+C\mathbf{H}_2CH_2$ groups yield triplets with $^3J = 6.6$ Hz ($n =$

(30) Braun, S.; Kalinowski, H.-O.; Berger, S. *100 and More Basic NMR Experiments, A Practical Course*, VCH: Weinheim, 1996.
(31) Katritzky, A. R.; Dega-Szafran, Z. *Magn. Reson. Chem.* **1989**, *27*, 1090−1105.

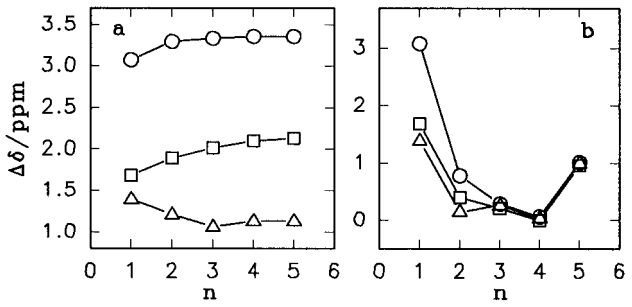

Figure 5. ^{1}H NMR chemical shift difference of the methylene protons between pyridinium alkanoates and sodium alkanoates (○), sodium phenylalkanoates (□), and sodium ω-bromoalkanoates (Δ), and as a function of the number of methylenes n in the zwitterion (a) $N^+C\mathbf{H}_2$ protons and (b) $C\mathbf{H}_2COO^-$ protons. Data are for D_2O solutes.

2) and 7.3 Hz (n = 3−5, 7, 10), respectively, indicating a free rotation about this bond. In alkylobetaines ($C_mH_{2m+1}(CH_3)_2N^+(CH_2)_nCOO^-$) multiplets with ^3J = 11.8−12.0 Hz and ^3J = 4.8−5.0 Hz have been observed for the $N^+C\mathbf{H}_2CH_2$ protons.[7] The appearance of two proton coupling constants suggests that the $N-CH_2$ bond is subject to hindered rotations, when the N^+ atom has four substituents.

In betaines the NMR chemical shift is affected by an electric field. A significant electric field dependent contribution to the ^{1}H chemical shift can be interpreted on the basis of polarization of the bonds between carbon and adjacent atoms by an electric field originating at a point charge, molecular dipole, or other intra- or intermolecular sources.[5,6,32] Thus, an electric charge introduced into a molecule creates an electric field that shifts all NMR resonance frequencies of its nuclei. It is clear that the more intense the field the larger the shifts, so that nuclei located close to the introduced electrical charge should be shifted more than those located farther away. The estimated intramolecular electric field effect for conformational analysis has been applied to some systems including zwitterions.[5,6,33] Information of intercharge distance of a zwitterion (the influence of the electric field due to one charge on the NMR resonance frequency of a nuclei located near the other one) can be obtained by measuring the chemical shift difference between two homologous compounds, one zwitterionic having both its charges and other one having one charge left, all the remaining part of molecule being kept constant. Figure 5 shows the ^{1}H NMR chemical shift difference of the methylene protons [$\Delta\delta = \delta$(PBn) − δ(X-$(CH_2)_n$COONa)] between pyridinium alkanoates and sodium alkanoates (X = Me), sodium ω-phenylalkanoates (X = Ph), and sodium ω-bromoalkanoates (X = Br) (the chemical shift variation upon replacement of methyl or phenyl groups or bromo atom of sodium alkanoates by charged pyridine ring was used in this study). Note, that the magnitudes of $\Delta\delta$ vary with compounds used as the model. The difference of chemical shifts between PBn and phenylalkanoates can be used as a measure of the positive charge effect on the chemical shift in betaines. The data collected in Figure 5 suggest that polymethylene chain has more gauche conformation than carboxylic acids.

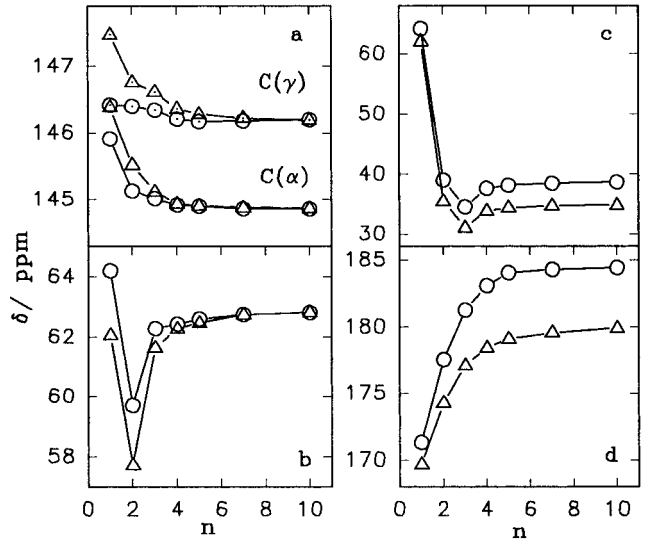

Figure 6. Effect of the polymethylene bridges length on the carbon-13 chemical shift of pyridine betaines (○) and their hydrobromides (Δ) in D_2O: (a) the pyridine ring carbon atoms, (b) $N^+{}^{13}\mathbf{C}H_2$, (c) $^{13}\mathbf{C}H_2COO^-$, and (d) COO. Data for hydrobromides are taken from ref 10.

^{13}C NMR Studies. The 2D heteronuclear shift correlated contour maps (HETCOR)[30] were used to identify resonances in the ^{13}C NMR spectra. The chemical shifts from 1D spectra are deposited and may be obtained on request. Quaternization of a pyridine ring shields the α-carbon atom and deshields the β and γ carbons. The upfield shift for the α-carbon atom has been assigned to change in the C−N bond order, and the β and γ shifts have been assigned to charge polarization effects.[34] The magnitude of these changes also depends on the substituent attached to the quaternary nitrogen atom; however, elongation of the carbon chain practically caused no effect.[32]

In the investigated pyridine betaines the COO group influences the chemical shifts of the ring α- and γ-carbon atoms (Figure 6a); their shifts decrease with elongation of the polymethylene chain separating the charged centers. Figures 6b and 6c show the chemical shift variations as a function of the number of intercharge methylenes units n in PBn for $N^+\mathbf{C}H_2$ and $\mathbf{C}H_2COO^-$ carbons, respectively. The $N^+\mathbf{C}H_2$ carbons are less upfield (4.49 ppm, n = 2) than the $\mathbf{C}H_2COO^-$ carbons (29.70 ppm, n = 3). Sensitive to the chain elongation are also the chemical shifts of the **C**=O carbon atoms (Figure 6d). The observed monotonic downfield shift of the **C**=O carbon atoms confirms that the interactions between the charged centers decrease when the tether becomes longer. Figure 7 shows that the ν_{as}COO frequency and the chemical shifts of the C=O carbon are modified by the positive nitrogen charged center in a comparable way; the straight line has a slope of −0.176(4), intercept of 458(6), and r = 0.999.

Figure 8 shows the ^{13}C NMR chemical shift difference ($\Delta\delta$, see above) of the carboxylate carbon between pyridinium alkanoates and sodium alkanoates,[5,35] sodium ω-phenylalkanoates, and sodium ω-bromoalkanoates (the

(32) Buckingham, A. D. *Can. J. Chem.* **1960**, *38*, 300−307.
(33) Batchelor, J. G.; Prestegard, J. H.; Cushley, R. J.; Lipsky, S. R. *J. Am. Chem. Soc.* **1973**, *95*, 6358−6364.
(34) Bolton, A. J.; McKillop, A. *Comprehensive Heterocyclic Chemistry*; Katritzky, A. R., Rees, C. W., Eds.; Pergamon Press: Oxford, 1984; Vol. 2, part 2A, p 1.
(35) Couperus, P. A.; Clagues, A. D. H.; van Dongen, J. P. C. M. *Org. Magn. Reson.* **1978**, *11*, 590−597.

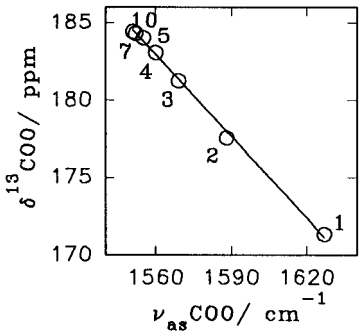

Figure 7. Correlation of the carbon-13 chemical shifts of the carboxylate group (δ) with the antisymmetric stretching vibration in D_2O of pyridine betaines.

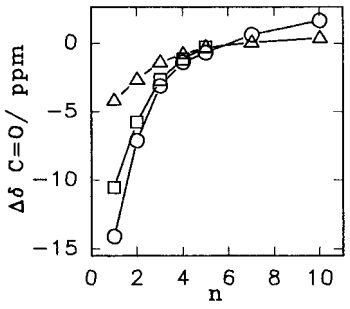

Figure 8. ^{13}C NMR chemical shift difference of the carboxylate carbon between pyridinium alkanoates and sodium alkanoates (○), sodium phenylalkanoates (□) and sodium ω-bromoalkanoates (Δ), as a function of the number of methylenes n in the zwitterion. Data are for D_2O solutes.

chemical shift variation upon replacement of methyl group or bromo atom of sodium alkanoates by charged pyridine ring was used in this study). Note that the magnitudes of $\Delta\delta$ vary with compounds used as the model. In the case of ω-bromoalkanoates the $\Delta\delta$ values are about three times smaller than those of normal alkanoates, as a consequence of the electric field of the dipole moment of $Br-CH_2$ bond. Similar $\Delta\delta$ values were observed for (trimethylammonio)alkanoates[5,6] and (*N*-dodecyl-*N*,*N*-dimethylammonio)alkanoates[6] when alkanoates were used as the model compounds. From those data Chevalier et al.[5,6] estimated the mean intercharge distance. The similar $\Delta\delta$ values suggest that the intercharge distances in pyridinium alkanoates are of similar magnitude with those of (trialkyloammonio)-alkanoates.

^{14}N NMR Studies. The nitrogen-14 chemical shift is little concentration dependent ($C_5H_5N^+CH_2COO^-$, −172.86 ppm, 0.1 mol dcm^{-3}; −172.87 ppm, 0.01 mol dcm^{-3}; −172.72 ppm, 0.001 mol dcm^{-3}). As Figure 9 shows a correlation of the nitrogen-14 chemical shifts with n is very similar to that in Figure 6d. However, contrary to the excellent linear correlation of the carbon-13 chemical shifts vs ν_{as}COO (Figure 8), the analogous plots of nitrogen-14 chemical shifts vs carbon-13 chemical shifts of **C**OO (Figure 10a; slope 0.44(5), intercept −247(9), r = 0.967) or vs ν_{as}COO (Figure 10b; slope −0.078(7), intercept −45(11), r = 0.977) are of little value. This is mainly caused by a deviation data for n = 2 from the straight lines.

PM3 and SAM1 Calculations. According to the results listed in Table 3, in the gas phase (as isolated molecules) the most stable are folded conformers pre-

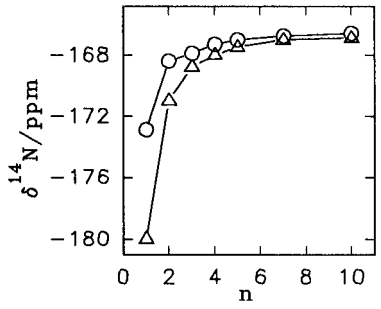

Figure 9. Effect of the polymethylene bridges length on the nitrogen-14 chemical shifts (δ) with the antisymmetric stretching vibration of pyridine betaines in D_2O (○) and 5% HCl (△).

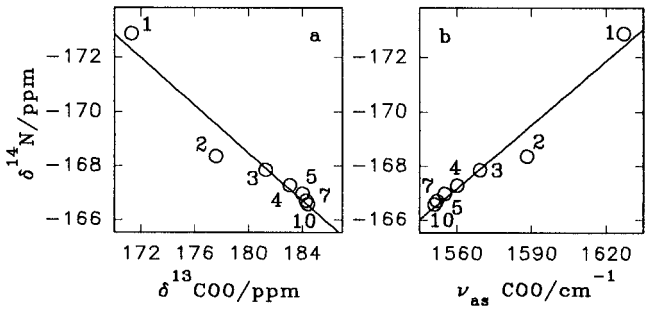

Figure 10. Correlation of the nitrogen-14 chemical shifts with the carbon-13 chemical shifts of the COO group (a) and with ν_{as}COO vibrations (b) of pyridine betaines in D_2O.

sented in Figures 11−13. The conformations of all investigated betaines in the gas phase are determined by intramolecular Coulombic attraction between the positive nitrogen atom and the negative oxygen atoms or chloride ion and also by the $O-H\cdots Cl^-$ (in PBn·HCl) or $O^-\cdots HOH$ (in PBn·$2H_2O$) hydrogen bonds. All conformers are arranged into cyclic species.

Changes of the relative energies (ΔH_f(folded) − ΔH_f(extended)) with n are plotted in Figure 14. These results suggest that electrostatic attraction between the two charged centers results in a folding of the intercharge arm when n exceeds 2.

The dipole moments for extended conformers increase as the tether length increases, which is consistent with the increased separation of the two charged localized regions. In contrast, the dipole moments for the folded conformers are almost independent of the tether length, in agreement with the essentially comparable distance for the intramolecular "ion-pair" in all folded conformations (Figure 15b).

The ΔH_f, μ, R($N^+\cdots C_c$) and R($N^+\cdots O_1$) values predicted by the PM3 and SAM1 methods are slightly different but vary in the same direction with n (Figure 15a, Table 3).

Carboxylic acids may have their hydroxyl proton either cis or trans to the C=O bond. The cis rotamer in formic acid was found to be 6.2 kcal mol^{-1} more stable than trans.[36] In the investigated hydrochlorides COOH group has trans conformation when $n = 1 \div 3$ and cis when $n = 4 \div 10$.

The electrostatic interactions decrease the proton-acceptor properties of the chloride ion, and consequently a proton transfer takes place in all PBn·HCl in the gas

(36) Hillenbrand E. A.; Scheiner, S. *J. Am. Chem. Soc.* **1986**, *108*, 7178−7186.

Table 3. PM3 and SAM1 Heats of Formation (kcal/mol), Dipole Moments (Debye), and Selected Distances (Å) between Nitrogen and Other Atoms for Betaines, PBn ≈ $C_5H_5N^+(CH_2)_nCOO^-$, and Their Dihydrates and Hydrochlorides

		PB1		PB2		PB3		PB4		PB5		PB7		PB10	
	method	PM3	SAM1	PM3	SAM1	PM3	SAM1	PM3	SAM1	PM3	SAM1	PM3	SAM1	PM3	SAM1
PBn	ΔH	−17.18	−22.74	0.23	−5.46	5.90	0.36	10.57	3.51	11.36	4.40	9.73	2.82	1.16	−4.27
extended	μ	12.93	11.95	20.42	19.57	25.65	24.83	32.81	31.86	37.98	37.38	48.40	49.75	61.46	68.66
(trans)	$R(N^+\cdots C_c)$	2.588	2.638	3.867	3.894	4.991	5.041	6.304	6.372	7.474	7.568	9.991	10.110	13.812	13.980
	$R(N^+\cdots O_1)$	2.912	2.914	4.356	4.117	5.162	5.118	6.842	6.935	7.882	7.986	10.501	10.596	14.327	14.500
PBn	ΔH	−17.18	−22.74	−16.91	−23.51	−22.09	−24.63	−30.07	−30.75	−37.92	−37.68	−50.57	−46.10	−71.07	−63.93
folded	μ	12.95	11.95	15.61	13.36	13.58	12.78	12.13	10.78	11.62	11.01	11.38	10.74	10.00	8.11
	$R(N^+\cdots C_c)$	2.588	2.638	3.356	3.316	3.506	3.532	3.563	3.490	3.728	3.846	3.885	4.029	3.994	3.879
	$R(N^+\cdots O_1)$	2.912	2.914	3.284	3.203	3.108	3.041	3.573	3.385	3.166	3.064	3.179	3.064	3.514	3.468
PBn·2H_2O	ΔH	−147.80	−156.88	−131.12	−142.26	−126.77	−142.49	−124.55	−134.59	−122.42	−134.59	−124.09	−136.35	−131.56	−142.77
extended	μ	10.20	8.97	21.29	19.90	23.78	24.24	28.86	28.50	38.36	37.92	50.75	50.98	70.05	71.34
(trans)	$R(N^+\cdots C_c)$	2.505	2.525	3.819	3.830	4.916	5.005	6.274	6.343	7.452	7.540	9.978	10.090	13.782	13.950
$\epsilon = 1$	$R(N^+\cdots O_1)$	3.182	3.213	4.423	4.294	5.211	5.017	6.772	6.778	7.675	7.737	10.379	10.475	14.226	14.453
PBn·2H_2O	ΔH	−147.80	−156.88	−139.00	−148.75	−150.78	−158.63	−155.57	−164.98	−164.99	−169.77	−176.77	−175.65	−189.09	−190.77
folded	μ	10.02	8.97	16.44	14.74	12.83	11.71	12.83	11.84	11.46	10.79	11.99	10.49	13.62	11.50
$\epsilon = 1$	$R(N^+\cdots C_c)$	2.505	2.525	3.787	3.787	3.454	3.799	4.017	4.069	4.144	4.196	4.280	4.600	4.219	4.219
	$R(N^+\cdots O_1)$	3.182	3.213	4.269	4.269	4.318	3.449	3.491	3.745	3.610	3.686	3.495	3.877	3.774	3.774
	$R(N^+\cdots OH_2)$	3.460	3.406	3.528	3.528	3.793	3.949	3.856	3.699	3.894	3.623	3.774	3.706	4.571	4.571
	$\angle O_2{-}C_c{-}O_1{\cdot}H$	175.10	174.79	161.15	143.46	27.07	44.96	−53.24	−43.85	−7.87	−2.39	−38.75	−23.66	33.75	50.89
	$\angle O_1{-}C_c{-}O_2{\cdot}H$	−174.08	−172.86	−154.53	−149.81	−78.09	−52.43	0.17	−2.22	−69.32	−122.71	−16.77	−32.45	−49.01	−53.50
PBn·2H_2O	a_o[a]	4.5	–	4.92	–	5.36	–	5.89	–	6.31	–	7.17	–	7.69	–
$\epsilon = 78$	ΔH	−166.42	–	−175.99	–	−176.83	–	−178.01	–	−180.89	–	−187.89	–	−225.13	–
	μ	22.49	–	32.11	–	37.55	–	43.50	–	49.36	–	61.00	–	80.14	–
	$R(N^+\cdots C_c)$	2.517	–	3.931	–	5.188	–	6.447	–	7.723	–	10.229	–	14.100	–
		2.48[b]		3.81[b]		4.50[b]		5.40[b]	–	6.15[b]		7.7[b]		(∼10)[b]	–
	$R(N^+\cdots O_1)$	3.244	–	4.374	–	5.458	–	6.789	–	7.971	–	10.768	–	14.310	–
	$R(N^+\cdots OH_2)$	3.489	–	6.955	–	7.927	–	9.081	–	10.345	–	13.078	–	16.702	–
	$\angle O_2{-}C_c{-}O_1{\cdot}H$	170.63	–	−0.53	–	−8.43	–	−4.13	–	−14.16	–	−3.08	–	−14.12	
	$\angle O_1{-}C_c{-}O_2{\cdot}H$	−129.04	–	−3.79	–	−12.49	–	7.35	–	−11.52	–	43.08	–	−1.13	
PBn·HCl	ΔH	−67.43	−71.95	−67.77	−67.39	−77.45	−80.27	−81.46	−78.65	−88.08	−93.39	−100.90	−101.64	−120.33	−117.26
folded	μ	11.10	10.64	11.47	10.72	14.63	13.69	9.92	7.84	13.43	13.22	14.18	13.52	13.21	12.54
	$R(N^+\cdots C_c)$	2.485	2.474	3.468	3.620	4.285	4.284	3.939	4.068	4.505	4.706	5.285	6.609	5.362	5.681
	$R(N^+\cdots O_1)$	3.347	3.337	3.857	3.978	4.454	4.437	3.600	3.665	3.941	3.875	4.601	5.559	4.078	4.412
	$R(N^+\cdots Cl)$	3.236	3.287	2.867	2.915	3.634	3.637	3.083	3.000	3.626	3.705	3.522	5.807	3.263	3.327
	$R(O_1{-}H)$	0.993	1.024	0.992	1.020	0.987	1.016	0.998	1.024	1.006	1.032	0.998	1.030	0.994	1.016
	$R(O_1\cdots Cl)$	2.755	2.837	2.733	2.817	2.767	2.834	2.719	2.744	2.680	2.727	2.697	2.739	2.717	2.798
	$\angle O_2{-}C_c{-}O_1{-}H$	177.39	177.72	−176.46	−177.14	172.28	171.10	−171.12	−176.17	−0.15	3.90	10.58	−0.10	9.19	6.37

[a] Cavity radius in Å. [b]Distances estimated for $(CH_3)_3N^+(CH_2)_nCOO^-$ taken from ref 5.

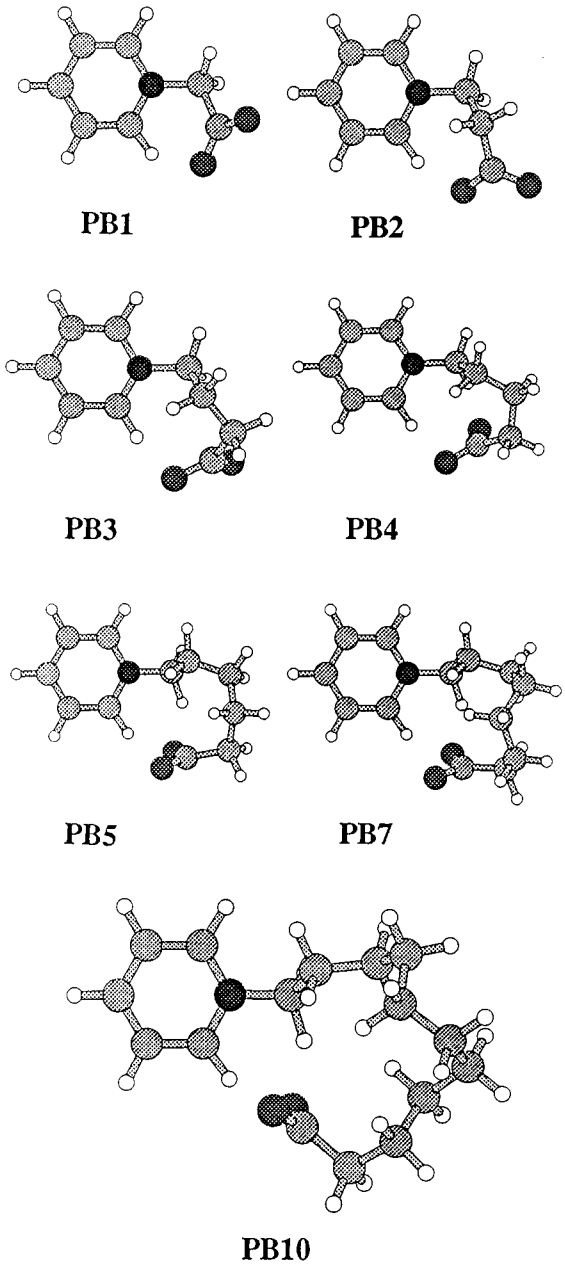

Figure 11. The PM3-optimized conformations of PBn.

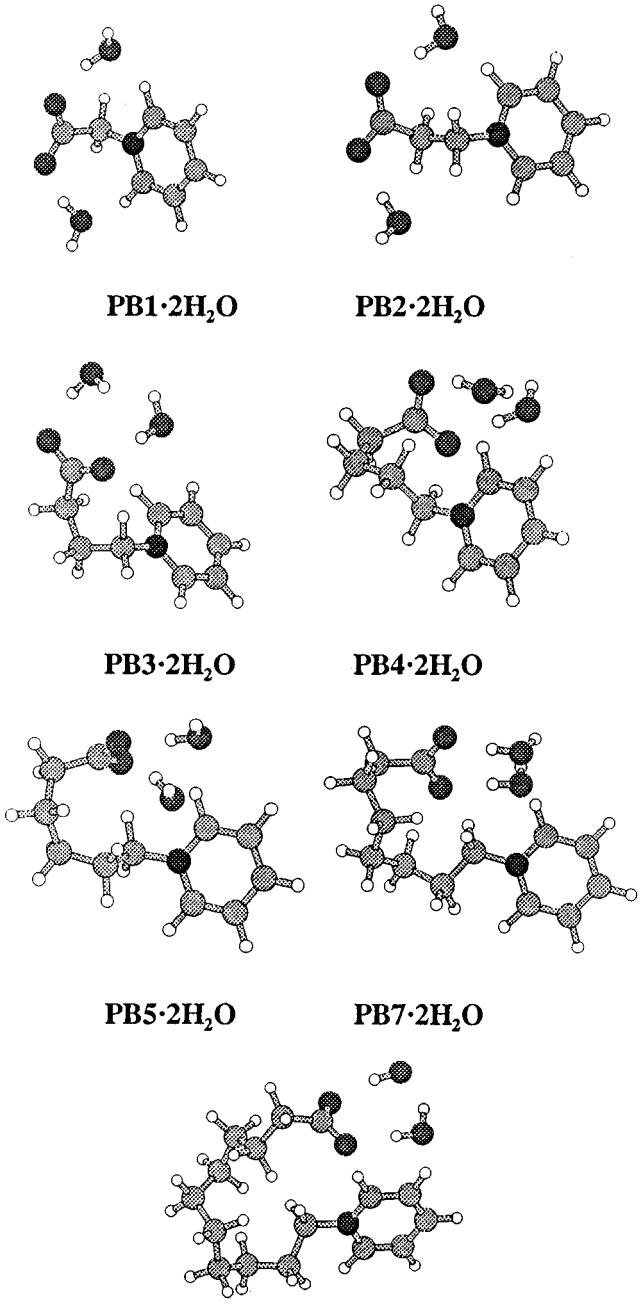

Figure 12. The PM3-optimized conformations of PBn·2H_2O.

phase. Aliphatic amines ($pK_a = 9.8 \div 10.8$) are much stronger bases than pyridine betaines ($pK_a = 1.73 \div 4.60$) and with hydrochloride in the gas phase form simple hydrogen bonded complexes ($R_3N\cdots HCl$), without proton transfer.[37]

The effect of solvents on the solute molecules may be categorized into specific and nonspecific classes as it is often possible to distinguish these two types of interactions by experimental methods.[38,39] Nonspecific interactions can arise from dispersion and electrostatic effects. In essence, the nonspecific influences are produced by electrostatic interactions between the charge distribution of the solute and solvent molecules, and this can be described, for example, by a moment expansion such as that given by Onsager reaction field theory.[40] Tapia and Goscinski[27a] developed a quantum mechanical self-consistent reaction field (SCRF) theory based upon interacting dipole moments. Since then this model has been applied to a number of problems studied by both semiempirical and ab initio MO theories.[41,42] When some degree of a dielectric screening is added to the calculations in the form of SCRF, the predicted conformers are very close to the extended ones (Table 3). The predicted

(37) Legon, A. C., *Chem. Soc. Rev.* **1993**, *22*, 153−163.
(38) Małecki, J. In *Molecular Interactions*; Ratajczak, H., Orville-Thomas, W. J., Eds.; Wiley: Chichester, U.K.; Vol. 3, 1982; pp 183−240.
(39) Reichardt, C. *Solvents and Solvate Effects in Organic Chemistry*, Verlag Chemie: Weinheim, 1988.
(40) Onsager, L., *J. Am. Chem. Soc.* **1936**, *58*, 1486−1493.
(41) Szafran, M.; Karelson, M. M.; Katritzky, A. R.; Koput, J.; Zerner, M. C. *J. Comput. Chem.* **1993**, *14*, 371−377 and ref cited therein.
(42) Tomasi, J.; Persico, M. *Chem. Rev.* **1994**, *94*, 2027−2094.

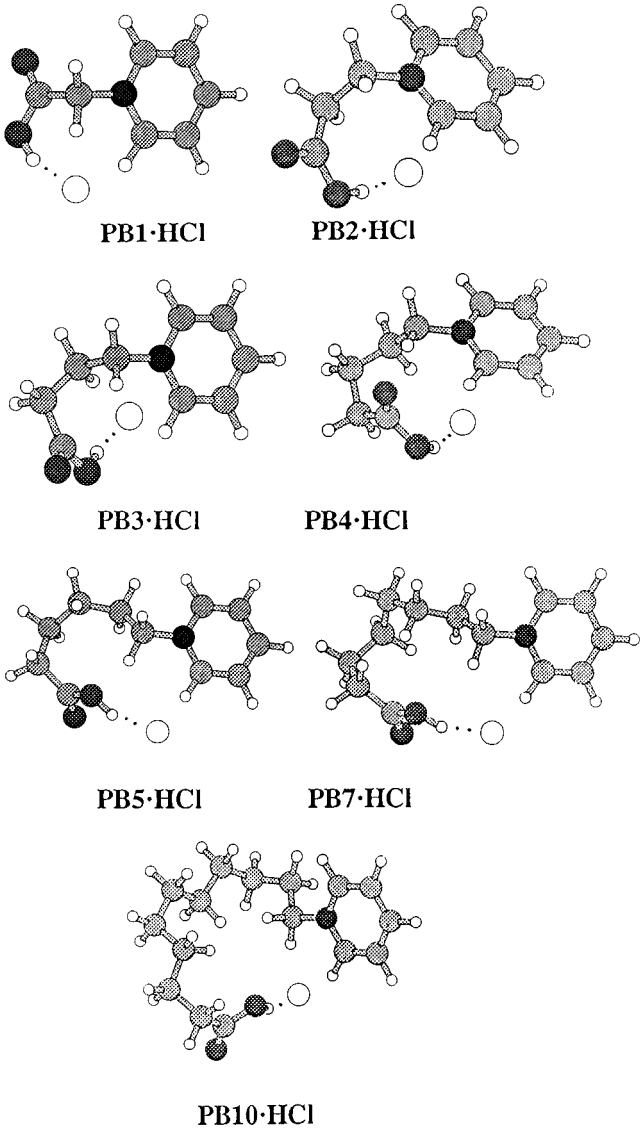

Figure 13. The PM3-optimized conformations of PBn·HCl.

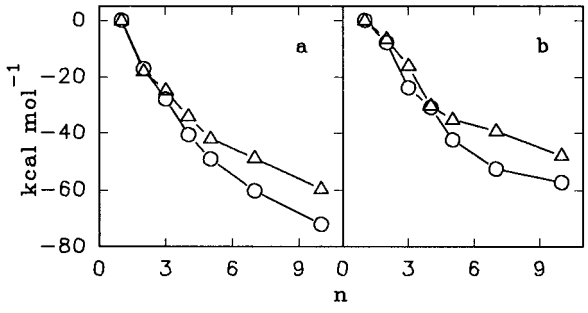

Figure 14. Isomerization energies (ΔH_f(folded) $-H_f$(extended)) (kcal·mol^{-1}) as a function of *n* (a) PBn, (b) PBn·2H_2O, (○) the PM3 data, (△) the SAM1 data.

intercharge distances are slightly longer than those estimated by Chevalier and Perchec[5] for (trialkylammonio)alkanocarboxylates ($Me_3N^+(CH_2)_nCOO^-$) from ^{13}C NMR spectra. Those differences and data presented in Figures 5 and 8 suggest that the SCRF model underestimates contribution of the gauche conformers.

BLYP Calculations. Selected BLYP data for PBn and PBn·HCl are listed in Table 4. The conformations

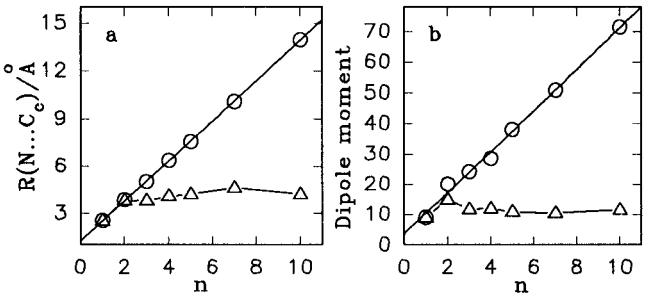

Figure 15. Effect of the polymethylene bridge lengths on the N···C_c distances (a) and the dipole moments (b) as calculated by the SAM1 method for pyridine betaines; (○) extended (trans), (△) folded.

predicted by BLYP calculations are slightly different than those from PM3 and SAM1 methods but comparable. Dipole moments predicted by the BLYP method for PB1, PB2, and PB3 are lower but for their hydrochlorides higher in comparison to those derived by semiempirical methods. In the case of PB4 and PB4·HCl the BLYP values are comparable with the PM3 data.

The optimized geometrical parameters for PB1 are deposited. The corresponding bond distances from the BLYP method are longer than those from X-ray diffraction except for the C(1)−N bond. The differences are probably caused by intermolecular interactions. It is well-known that intermolecular interactions may cause the molecular geometry in the crystal to be different from that of the free molecules.[43]

Conclusions

Conformation of flexible zwitterionic betaines is stabilized by the electrostatic interaction between the charged centers and hydrogen bonding. Linear molecules in crystals are arranged antiparallel with short intermolecular contacts between the N^+ and COO^- groups. Water molecules form hydrogen bonds with the COO^- group and additionally stabilized linear structures. Methylene groups in PB3·2H_2O and PB10·3H_2O form a *trans*-zigzag pattern, while PB1 and PB1·H_2O have conformations with one of the oxygen atoms located closer to the N^+ atom.

The results of FTIR and ^1H, ^{13}C, and ^{14}N NMR studies suggest that in aqueous solutions the intercharge distance increases with the increasing tether length due to the solvent effect, and in consequence the investigated structures are extended with some contribution of gauche conformers. Conclusive FTIR evidence comes from the decreasing $\nu_{as}COO^-$ frequencies with increasing *n*. This reflects an increase of symmetry of carboxylate groups caused by an increased distance from the N^+ atom. Further evidences are derived from a clear variation of the chemical shifts with *n* in the NMR spectra in aqueous solutions. In particular the downfield shifts of the ^{13}COO and ^{14}N atoms with *n*, the linear correlations presented in Figures 7 and 10, and the SCRF data listed in Table 3 confirmed extended structures in aqueous solutions. On the other hand, Figures 5 and 8 suggest that polymeth-

(43) (a) Hargittai, I. *Pure Appl. Chem.* **1989**, *61*, 651−660. (b) Chiang, J. F.; Song, J. J. *J. Mol. Struct.* **1982**, *96*, 151−162. (c) Katrusiak, A.; Kałuski, Z. In *Proceedings−Third Symposium on Organic Crystal Chemistry*, Poznań, Poland, 1980, Kałuski, Z., Ed. Adam Mickiewicz University Press: Poznań, 1980; pp 176−189.

Table 4. Selected BLYP/6-31G(d,p) Data for Folded PBn and PBn·HCl[a]

	PB1	PB1·HCl	PB2	PB2·HCl	PB3	PB3·HCl	PB4	PB4·HCl
E	−475.98551	−936.79867	−515.26020	−976.08553	−554.54676	−1015.37204	−593.82641	−1054.66534
μ	8.93	11.45	11.76	14.43	12.74	15.63	12.45	9.43
$R(N^+\cdots C_c)$	2.600	2.486	3.319	3.885	3.785	4.984	3.509	4.107
$R(N^+\cdots O_1)$	2.800	3.020	3.215	4.425	3.322	5.148	3.384	3.929
$R(N^+\cdots Cl^-)$	–	3.755	–	3.804	–	3.838	–	3.596
R(O−H)	–	1.051	–	1.022	–	1.012	–	1.018
$R(O\cdots Cl^-)$	–	2.949	–	3.056	–	3.132	–	3.018

[a] E in au; μ in Debye; R in Å.

ylene chains in PBn contain more folded conformers than the respective carboxylic acids.

All of these data suggest that methylene groups of PBn in aqueous solutions have either the trans and gauche conformations, but the former are in the majority.

Quite different conformations appear in the case of a single molecule. On going from condensed phase (the solid state and aqueous solution) to the gas phase the intermolecular electrostatic interactions are replaced by the intramolecular ones. Thus the calculated dipole moments and intramolecular distances between the charged groups for the single molecules are practically independent of n. The electrostatic interaction of the chloride ion with the positive nitrogen atom decreases the proton-acceptor properties of chloride ion and favors proton transfer in the gas phase.

Acknowledgment. This work was supported by the State Committee of Scientific Research (KBN), grant 2P 303 06907. Most of the calculations were done at the Poznań Supercomputing and Network Centre.

Supporting Information Available: Tables of X-ray and BLYP/6-31G(d,p) atomic coordinates, X-ray isotropic and anisotropic displacement parameters, bond lengths, angles, dihedral angles for PB1, PB1·H_2O, PB3·$2H_2O$, and PB10·$3H_2O$; ^1H, ^{13}C, and ^{14}N chemical shifts and IR frequencies for PBn; ^1H chemical shifts of the selected methylene groups in sodium ω-bromoalkanoates and sodium ω-phenylalkanoates in D_2O; and Z-matrices (40 pages). This material is contained in libraries on microfiche, immediately follows this article in the microfilm version of the journal, and can be ordered from the ACS; see any current masthead page for ordering information.

JO9720694